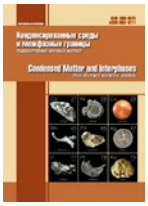

ISSN 1606-867X (Print)
ISSN 2687-0711 (Online)
Condensed Matter and Interphases
Kondensirovannye Sredy i Mezhfaznye Granitsy
https://journals.vsu.ru/kcmf/

Review

Review article
https://doi.org/10.17308/kcmf.2024.26/12384

Functional borates and their high-pressure polymorphic modifications. Review

T. B. Bekker[1,2]✉, A. V. Davydov[1,2], N. E. Sagatov[1,2]

[1]*V. S. Sobolev Institute of Geology and Mineralogy of the Siberian Branch of the Russian Academy of Sciences, 3 Ac. Koptyuga ave., Novosibirsk 630090, Russian Federation*

[2]*Novosibirsk State University 1 Pirogova st., Novosibirsk 630090, Russian Federation*

Abstract

The article presents the results of many years of studies of the growth of a low-temperature modification of barium borate β-BaB_2O_4 (*R*3*c*) crystals in the Na, Ba, B // O, F quaternary reciprocal system. Barium borate β-BaB_2O_4 is the most important nonlinear optical crystal of the UV spectrum. The key factor determining the quality of crystals is the choice of an optimal solvent. The article presents phase diagrams and the results of the growth of β-BaB_2O_4 crystals in several subsystems of the studied quaternary reciprocal system. Using atomistic modeling, we predicted and then experimentally obtained new high-pressure modifications: γ-BaB_2O_4 ($P2_1/n$), whose structure includes edge-sharing tetrahedra, and d-BaB_2O_4 with assumed symmetry $Pa\bar{3}$. In our study, we also focused on a solid solution with an "antizeolite" structure, which also crystallizes in the Na, Ba, B // O, F system.

Keywords: Low-temperature modification of barium metaborate, Quaternary reciprocal system, High-temperature solution growth, Borates with "antizeolite" structure

***Funding*:** The study was supported by the Russian Science Foundation grant No. 24-19-00252, https://rscf.ru/project/24-19-00252/

For citation: Bekker T. B., Davydov A. V., Sagatov N. E. Functional borates and their high-pressure polymorphic modifications. Review. *Condensed Matter and Interphases*. 2024;26(4): 620–632. https://doi.org/10.17308/kcmf.2024.26/12384

Для цитирования: Беккер Т. Б., Давыдов А. В., Сагатов Н. Е. Функциональные бораты и их высокобарические полиморфные модификации. Обзор. *Конденсированные среды и межфазные границы*. 2024;26(4): 620–632. https://doi.org/10.17308/kcmf.2024.26/12384

✉ Tatyana B. Bekker, e-mail: bekker@igm.nsc.ru, t.b.bekker@gmail.com

1. Introduction

Modifications of barium metaborate, α-BaB_2O_4 ($R\bar{3}c$) and β-BaB_2O_4 ($R3c$), are important materials with birefringent and nonlinear optical properties in the UV and visible spectra respectively. Low-temperature non-centrosymmetric modification β-BaB_2O_4 is widely used for the generation of the fourth and fifth harmonics of $Y_3Al_5O_{12}$:Nd^{3+} lasers (266 and 213 nm respectively), and as optical parametric generators and amplifiers [1–4]. β-BaB_2O_4 crystals are characterized by a wide transparency range (from 185 to 2500 nm), high nonlinear optical susceptibility (d_{22} (1064 nm) = 2.2 pm/V, d_{22} = 5.7d_{36} (KDP), an acceptable birefringence value (Δn = 0.113 (1064 nm)), a low light dispersion in the range from 204 to 1500 nm, and good physical and chemical properties [5].

The melting point of the high-temperature modification α-BaB_2O_4 is 1100 °C. Due to the α-β phase transition at a temperature of 925 °C the main method of growing β-BaB_2O_4 crystals is the high-temperature solution growth method, which ensures crystallization before the phase transition temperature is reached. The key factor determining the actual structure and optical quality of crystals is the choice of an optimal solvent. Earlier we suggested combining the main solvents used for the growth of β-BaB_2O_4 crystals, namely Na_2O [6] and components of the BaO–Na_2O–B_2O_3 ternary system [7–9], NaF [10–13] and BaF_2 [14, 15, 16], into a single quaternary reciprocal system Na, Ba, B // O, F [1, 17, 18]. Composition diagrams of quaternary reciprocal systems containing six salts A, B, C // X, Y are presented as a trigonal prism according to Jänecke [19]. A polytope of the Na, Ba, B // O, F system is shown in Fig. 1. The compositions of individual phases are presented in Table 1. Presented below are the results of the growth of β-BaB_2O_4 crystals performed using six solvents and the results of the synthesis of two new polymorphic modifications of BaB_2O_4 at high temperatures and pressures.

The Na, Ba, B // O, F system also includes a composition range of the solid solution of borates with an "antizeolite" structure. The structure of the solution is based on the $\{Ba_{12}(BO_3)_6\}^{6+}$ framework with channels along the *c* axis built of barium cubes and anticubes. The general formula of the solid solution in *this system* can be presented as $\{Ba_{12}(BO_3)_6\}[(F_2)_x(BO_3)_{1-x}][(F_4)_x(NaF_4)_y(BO_3)_{1-x-y}]$, where $x + y \leqslant 1$, and $[(F_2)_x(BO_3)_{1-x}]^{3-}$ and $[(F_4)_x(NaF_4)_y(BO_3)_{1-x-y}]^{3-}$ – are anionic groups in the barium anticubes and cubes, respectively. Fig. 1 shows a crosshatched triangle whose vertices contain experimentally determined phases: $Ba_3(BO_3)_2$, $\{Ba_{12}(BO_3)_6\}[BO_3][BO_3]$, x = 0, y = 0 [23], $Ba_3(BO_3)_{1.8}F_{0.6}$, $\{Ba_{12}(BO_3)_6\}[(F_2)_{0.4}(BO_3)_{0.6}][(F_4)_{0.4}(BO_3)_{0.6}]$, $x = 0.4, y = 0$ [24] and $NaBa_{12}(BO_3)_7F_4$, $\{Ba_{12}(BO_3)_6\}[BO_3][NaF_4]$, x = 0, y = 1 [22]. The $NaBa_{12}(BO_3)_7F_4$ phase was first described in [25] as having a centrosymmetric *I*4/*mcm* structure.

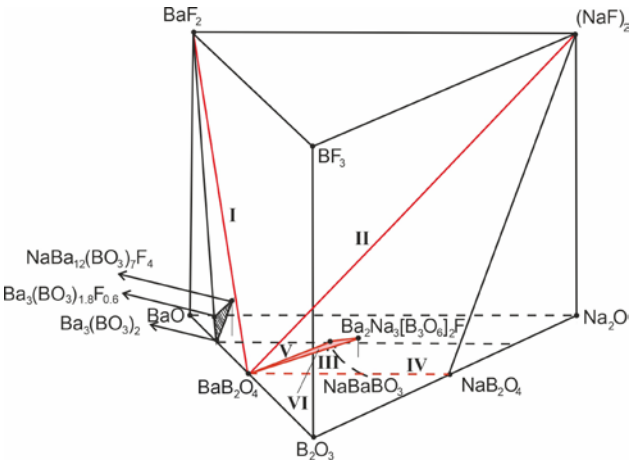

Fig. 1. Polytope of the quaternary reciprocal system Na, Ba, B // O, F. Subsystems used for growing β-BaB_2O_4 crystals: I BaB_2O_4–BaF_2, II BaB_2O_4–$(NaF)_2$, III BaB_2O_4–$Ba_2Na_3[B_3O_6]_2F$, IV BaB_2O_4 – $(NaBO_2)_2$, V BaB_2O_4 – 30 $NaBaBO_3$, VI 70BaB_2O_4 – $NaBaBO_3$ – $Ba_2Na_3[B_3O_6]_2F$

Table 1. Compositions of individual phases of the quaternary reciprocal system Na, Ba, B // O, F

Chemical formula	Compositions, mol %				Syngony, sp. gr., Z	Reference
	BaO	Na_2O	B_2O_3	BaF_2		
$NaBaBO_3$	50	25	25	–	Monoclinic, *C*2/*m*, 4	[20]
$Ba_2Na_3[B_3O_6]_2F$	23.1	23.1	46.1	7.7	Hexagonal, $P6_3/m$, 2	[21]
$NaBa_{12}(BO_3)_7F_4$	62.5	3.1	21.9	12.5	Tetragonal, $P4_2bc$, 4	[22]

However, this was not confirmed by the results of our X-ray structural analysis [22]. In this article we briefly describe the conditions for the growth of the $NaBa_{12}(BO_3)_7F_4$ phase and analyze the stability of the $Ba_3(BO_3)_{1.8}F_{0.6}$ phase at high temperatures and pressures.

2. Experimental research methods

2.1. High-temperature solution growth of β-BaB_2O_4 and NaBa12(BO3)7F4 crystals

β-BaB_2O_4 crystals were grown from high-temperature solutions in a top seed solution growth (TSSG) furnace. The compositions of the used high-temperature solutions I–VI are given in Table 2.

The starting materials were commercially available extra pure reagents $BaCO_3$, Na_2CO_3, H_3BO_3, NaF, and BaF_2. The initial batch weighing about 2 kg, whose composition corresponded to those presented in Table 2, was prepared by means of solid-phase synthesis and then melted in a platinum crucible (standard diameter of 80 and 100 mm). After determining the equilibrium temperature, a crystal seed was placed in contact with the top surface of the high-temperature solution; the seed was oriented along the optical axis and had a cross-section of 5×5 mm^2. The crystals were grown by constantly revolving the seed at a speed of 1 r/min. The cooling and pulling rates varied from 0.4 to 2 °C/day and from 0.5 to 0.1 mm/day respectively. In order to use the solution multiple times, β-BaB_2O_4 was added after each growth cycle obtained by means of solid-phase synthesis from metaboric acid HBO_2 and barium carbonate $BaCO_3$. The weight of the added β-BaB_2O_4 corresponded to the weight of the grown crystals.

$NaBa_{12}(BO_3)_7F_4$ crystals were grown from 38 mol % BaO, 36 mol % BaF_2, 13 mol % B_2O_3, and 13 mol % Na_2O compositions; the starting materials were the same commercially available reagents as used for the growth of β-BaB_2O_4 crystals. After the solid-phase synthesis, the batch (300 g) was melted in a platinum crucible (diameter 60 mm). To grow the crystals, a crystal seed was used oriented along the [001] axis with constant pulling (0.3 mm/day) and revolving (1 r/min). The weight of the grown crystal was about 30 g.

2.2. Synthesis at high temperatures and pressures

Based on the ab initio calculations, we predicted the existence of two high-pressure polymorphic modifications of BaB_2O_4, which we denoted as γ-BaB_2O_4 and δ-BaB_2O_4. These modifications are stable under pressures above 0.9 GPa and 6.1 GPa respectively [14]. According to the calculations, δ-BaB_2O_4 is isostructural to CaB_2O_4 – $Pa\bar{3}$ [15].

We synthesized the new high-pressure modification γ-BaB_2O_4 using a Discoverer-1500 multi-anvil hydraulic press of the DIE type at a pressure of 3 GPa and a temperature of 900 °C [26]. The experiment lasted 24 hours. The anvils were 26 mm cubes of tungsten carbide. The medium of pressure transmission was semi-sintered ceramics ZrO_2 in the shape of an octahedron with the edge of 20.5 mm. Conducting another experiment at a pressing force of 6 GPa, which is the maximum pressure for the hydraulic press used, and a temperature of 900 °C for 48 hours, we also obtained the phase γ-BaB_2O_4. In both experiments the initial samples were

Table 2. Characteristics of high-temperature solutions used for growing β-BaB_2O_4 crystals

№	Compositions (mol %)	Na (wt. %)	ΔT_{theor} (°C)	K_{theor} / K_{exp} (g/(kg·°C))	Reference
I	54.5 BaB_2O_4 – 45.5 BaF_2	–	165	1.58 / 1.05,0.72	[18, 39]
II	79.9 BaB_2O_4 – 20.1 $(NaF)_2$ 60 BaB_2O_4 – 20 $Ba_2Na_3[B_3O_6]_2F$ – 20 BaF_2	**4.75**	125	3.63 / 2.76,2.02	[13]
III	60 BaB_2O_4 – 40 $Ba_2Na_3[B_3O_6]_2F$	**7.22**	100	3.09 / 2.85,2.39	[39, 30]
IV	70 BaB_2O_4 – 30 $(NaBO_2)_2$	**7.05**	94	3.83 / 3.22,3.20	[34, 35]
V	70 BaB_2O_4 – 30 $NaBaBO_3$	**3.11**	115	2.49 / 1.89,1.60	[40]
VI	70BaB_2O_4 – 22.5$NaBaBO_3$ – 7.5$Ba_2Na_3[B_3O_6]_2F$	**4.09**	120	2.80 / 2.2,2.03	[18, 39]

polycrystalline β-BaB_2O_4 obtained by means of solid-phase synthesis.

Up to the present moment, the fourth modification δ-BaB_2O_4 has only been obtained as a product of decomposition of barium-sodium metaborate $Ba_2Na_3(B_3O_6)_2F$ in an experiment conducted at a pressure of 6 GPa and a temperature of 900 °C for 64 hours [27]. The initial sample was a grounded $Ba_2Na_3(B_3O_6)_2F$ crystal.

The stability of the $Ba_3(BO_3)_{1.8}F_{0.6}$ phase was analyzed at 3 GPa and 1000 °C for 5 hours. The initial sample was a grounded $Ba_3(BO_3)_{1.8}F_{0.6}$ crystal.

During all the experiments, polycrystalline samples were put into holes in graphite cassettes. The diameter of the holes was 0.9 mm and the depth was 1.1 mm. Each sample was covered with an individual graphite lid. The temperature gradient between the low-temperature (LT) and high-temperature (HT) regions of the samples at 900 °C was about 5°C. The design of the high-pressure cell was detailed in [28].

2.3. Analytical research methods

The samples synthesized at high temperatures and pressures were filled with epoxy resin and polished. Due to the small size of the synthesized samples, whose crystals are usually no bigger than tens of micrometers, the main analysis method was scanning electron microscopy (MIRA 3 LMU, Tescan Orsay Holding) using an INCA 450 energy-dispersive microanalysis system with a large area EDS X-Max-80 Silicon Drift Detector.

Raman spectroscopy was also used to determine the composition and the polymorphic modification of each phase. Raman spectra were registered using a Horiba Jobin Yvon LabRAM HR800 spectrometer with a 1024-pixel LN/CCD detector. The wavelength of the Nd-YAG laser was 532 nm. Raman spectra were measured in the backscattering geometry using an Olympus BX41 microscope. The spectral resolution was ~2.0 cm^{-1}. The microscope with an Olympus 100× lens, WD = 0.37 mm with a numerical aperture for the visible spectrum had a focal diameter of ~2 μm. The power of laser radiation was 0.5 mW to prevent the heating of the sample.

The study was conducted using the equipment of the Centre for Collective Use of Scientific Equipment of the Institute of Geology and Mineralogy of the Siberian Branch of the Russian Academy of Sciences.

3. Results and discussion

3.1. Growth of β-BaB_2O_4 and $NaBa_{12}(BO_3)_7F_4$ crystals

Presented below is a brief description of the six systems used for the growth of β-BaB_2O_4 crystals (Table 2). Besides the compositions of the initial high-temperature solutions, Table 2 presents some additional characteristics, namely the concentration of sodium in the initial high-temperature solution, theoretical crystallization intervals (ΔT_{theor}), and theoretical and experimental yield coefficients (K_{theor} / K_{exp}). Theoretical crystallization interval (ΔT_{theor}) is a temperature range corresponding to the region of primary crystallization of β-BaB_2O_4 in the system. The theoretical yield coefficient (K_{theor}) is the difference (in grams) in the concentration of BaB_2O_4 in 1 kg of the high-temperature solution in the compositions limiting the region of primary crystallization of β-BaB_2O_4 divided by the theoretical crystallization interval. Therefore, the yield coefficient is measured in g/(kg×°C). Both parameters (the theoretical crystallization interval and the theoretical yield coefficient) are determined based on the phase diagram of the system. The experimental yield coefficient is determined as the weight of the grown crystal divided by the weight of the initial high-temperature solution and by the crystallization interval specific for each experiment.

I BaB_2O_4 – BaF_2. The melting point of BaF_2 is 1353 °C. The coordinates of the eutectic points are 41 mol % BaB_2O_4, 59 mol % BaF_2, 760 °C [18], the theoretical yield coefficient is 1.58 g/(kg×°C). A significant difference between the experimental and theoretical yield coefficients, as well as the drop of the experimental coefficient from 1.05 to 0.72 g/(kg×°C) in three consequent experiments can be explained by a rapid pyrohydrolysis of barium fluoride. During the third consequent experiment, co-crystallization of phases β-BaB_2O_4 and $Ba_5B_4O_{11}$ took place, which can be described by the following reactions:

$$BaF_2 + H_2O \rightarrow BaO + 2HF\uparrow \quad (1)$$

$$2BaB_2O_4 + 2BaO \rightarrow Ba_5B_4O_{11}. \quad (2)$$

II BaB_2O_4 – $(NaF)_2$. The study determined that the BaB_2O_4 – $(NaF)_2$ system is not chemically stable, which is completely different from the results obtained in [10]. A chemical reaction occurs between BaB_2O_4 and NaF [13, 29], which results in the formation of barium-sodium borate fluoride $Ba_2Na_3[B_3O_6]_2F$ ($P6_3/m$) [21], available for the study of phase equilibria in the system. The second product of the chemical reaction is barium fluoride:

$$79.9\ BaB_2O_4 + 20.1\ (NaF)_2 \rightarrow$$
$$\rightarrow 13.4\ Ba_2Na_3[B_3O_6]_2F + 13.4\ BaF_2 + 39.7\ BaB_2O_4 \quad (3)$$

$$66.7\ BaB_2O_4 + 33.3\ (NaF)_2 \rightarrow$$
$$\rightarrow 22.2\ Ba_2Na_3[B_3O_6]_2F + 22.2\ BaF_2 \quad (4)$$

Thus, the initial composition 79.9 mol % BaB_2O_4, 20.1 mol % $(NaF)_2$ transforms into a composition 20 mol % $Ba_2Na_3[B_3O_6]_2F$, 20 mol % BaF_2, 60 mol % BaB_2O_4 during the solid-phase synthesis at 720 °C, which is demonstrated in Table 2. The region of primary crystallization of β-BaB_2O_4 in the system is limited by the composition 66.7 mol % BaB_2O_4, 33.3 mol % $(NaF)_2$, when BaB_2O_4 and $(NaF)_2$ react completely according to (4), which results in the formation of $Ba_2Na_3[B_3O_6]_2F$ and BaF_2 (Fig. 2a). This composition was used to grow a $Ba_2Na_3[B_3O_6]_2F$ crystal [13], whose image is given in the insert to Fig. 2a. We should note that the composition of $Ba_2Na_3[B_3O_6]_2F$ is not on the BaB_2O_4 – $(NaF)_2$ section. It belongs to the Na, Ba // BO_2, F ternary reciprocal system, which was detailed in [29].

The crystallization interval of β-BaB_2O_4 is 125 °C. The drop in the experimental yield coefficient from 2.76 to 2.02 g/(kg×°C) in three consequent experiments can be accounted for by the pyrohydrolysis of barium fluoride formed in the system. An image of the β-BaB_2O_4 crystal grown in the system is presented in the insert to Fig. 2a.

III BaB_2O_4 – $Ba_2Na_3[B_3O_6]_2F$. The $Ba_2Na_3[B_3O_6]_2F$ compound melts congruently at 835 °C. The coordinates of the eutectic points of the system are 85 mol % $Ba_2Na_3[B_3O_6]_2F$, 15 mol % BaB_2O_4, 810 °C [30]. The system is characterized by a relatively high theoretical yield coefficient of 3.09 g/(kg×°C). The experimental yield coefficient in three consequent cycles changed from 2.85 to 2.39 g/(kg×°C). The phase diagram and an image of the crystal grown in the system are presented in Fig. 2b.

IV BaB_2O_4 – $(NaBO_2)_2$. The melting point of $NaBO_2$ is 997 °C. The coordinates of the eutectic points of the system are 44 mol % $(NaBO_2)_2$, 56 mol % BaB_2O_4, 831 °C [31]. The crystallization interval of β-BaB_2O_4 is 94 °C and the theoretical yield coefficient is 3.83 g/(kg×°C). The system is

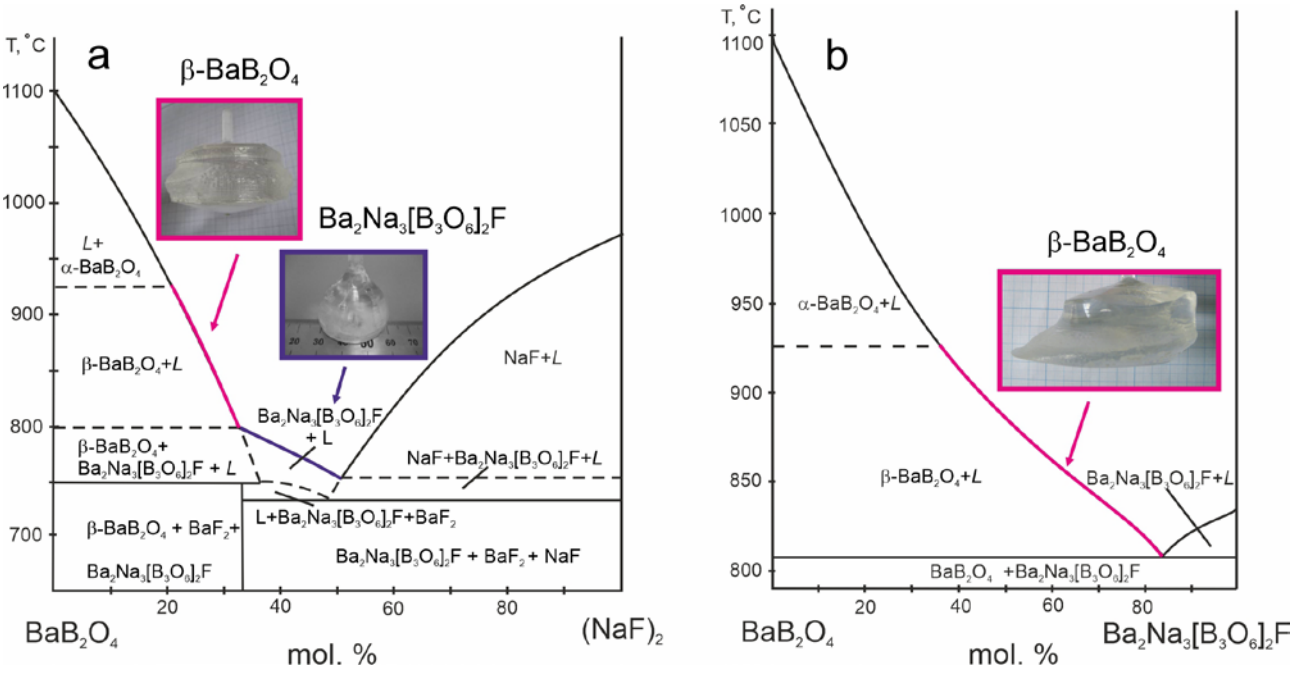

Fig. 2. Phase diagrams of the BaB_2O_4 - $(NaF)_2$ (a) and BaB_2O_4 - $Ba_2Na_3[B_3O_6]_2F$ (b) systems and photographs of crystals grown in these systems

characterized by the highest experimental yield coefficient of 3.22 g/(kg×°C).

V BaB_2O_4 – $NaBaBO_3$. The $NaBaBO_3$ (*C*2/*m*) compound [20] melts congruently at 1270 °C. It was determined that the BaB_2O_4–$NaBaBO_3$ system is quasi-binary only in the solid state, i.e. at temperatures below 760 °C, and crosses the region of primary crystallization of $Ba_5B_4O_{11}$ [32] and $NaBa_4(BO_3)_3$ [33]. The crystallization interval corresponding to the region of primary crystallization of β-BaB_2O_4 (Fig. 3) is 115 °C and the theoretical yield coefficient is 2.49 g/(kg×°C). The experimental yield coefficient varies in the range of 1.89÷1.60 g/(kg×°C).

VI BaB_2O_4 – $NaBaBO_3$ – $Ba_2Na_3[B_3O_6]_2F$. The composition used for the growth of β-BaB_2O_4 in this ternary system is 70 mol % BaB_2O_4, 22.5 mol % $NaBaBO_3$, and 7.5 $Ba_2Na_3[B_3O_6]_2F$ mol %. The crystallization interval of β-BaB_2O_4 is 120 °C and the theoretical yield coefficient is 2.80 g/(kg×°C). The experimental yield coefficient is 2.20 g/(kg×°C).

One of the key characteristics determining the possibility of using optical elements based on β-BaB_2O_4 crystals in laser systems is the absence of scattering, when laser radiation passes through a crystal. We assume that the formation of scattering centers in β-BaB_2O_4 crystals is associated with the introduction of sodium impurities. The concentration of sodium in the initial high-temperature solution is presented in Table 2. Inductively coupled plasma atomic emission spectroscopy demonstrated that the concentration of sodium in crystals is lower by at least three orders of magnitude [34, 35]. Sodium ions can be incorporated both into barium positions and into interstitial sites [36–38].

Despite the rapid pyrohydrolysis and a drop in the yield coefficient, crystals grown in system I did not scatter the laser beam. During long-term storage, the crystals were split by cleavage, which can be a result of thermoelastic relaxation. Crystals grown in systems II and III (the concentration of Na in the initial solutions was 4.75 wt. % and 7.22 wt. % respectively) appeared to be of good quality. However, they demonstrated laser beam scattering in the entire volume. Crystals obtained in system IV (7.05 wt. % Na) contained solid-phase inclusions of up to 200 μm; the regions without inclusions also

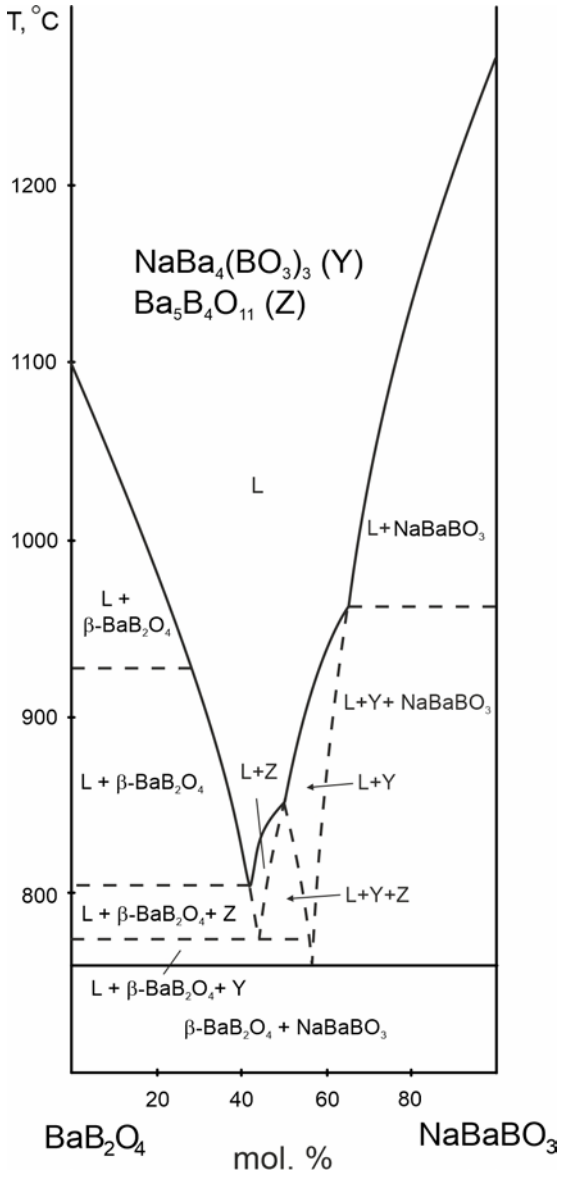

Fig. 3. Phase diagram of the BaB_2O_4 - $NaBaBO_3$ system

demonstrated laser scattering. Crystals grown in system V (3.11 wt. % Na) did not scatter laser beams, which was confirmed be a few dozen experiments. The disadvantages of the system are a low yield coefficient and a loss of stability of the crystallization front at a certain point resulting in cellular growth. The crystals of system VI (4.09 wt. % Na) were also characterized by a high optical quality and a higher experimental yield coefficient than the crystals of system V. We should note that in the consequent experiments with system VI the yield coefficient changed insignificantly, which can be explained by the absence of free barium fluoride susceptible to

pyrohydrolysis in the initial composition. At the same time, the presence of borate fluoride $Ba_2Na_3[B_3O_6]_2F$ apparently helps to reduce the viscosity of the high-temperature solution.

Fig. 4 demonstrates an image of the $NaBa_{12}(BO_3)_7F_4$ crystal, the end member of the solid solution with an "antizeolite" structure grown in the Na, Ba, B // O, F system. The crystal presented in Fig.4 is dark crimson. Another formally colorless group of compounds that were first classified as "antizeolites", are compounds of the meionite group $Ca_{12}Al_{14}O_{33}$ [41-44]. The color of the $NaBa_{12}(BO_3)_7F_4$ crystals grown in the Na, Ba, B // O, F system is determined by the concentration of intrinsic defects and depends on the composition of the initial high-temperature solution [45]. The crystals are characterized by *linear dichroism*, i.e. different light absorption depending on the orientation of the light-wave vector, which makes it possible to use them as polarizers in optical systems [46]. It was also determined that depending on the composition of the initial high-temperature solution, the dielectric permeability of the $NaBa_{12}(BO_3)_7F_4$ crystals changes by an order of magnitude and becomes unusually high for borate crystals (319(5)) [47].

Fig. 4. Photograph of a crystal $NaBa_{12}(BO_3)_7F_4$ ($P4_2bc$), 28×28×11 mm, grown in the system Na, Ba, B // O, F from a composition of 38 mol % BaO, 13 mol % Na_2O, 13 mol % Ba_2O_3, 36 mol % BaF_2

3.2. Synthesis at high temperatures and pressures

As an initial sample in our experiment we used polycrystalline β-BaB_2O_4 obtained by means of solid-phase synthesis. At 3 GPa and 900 °C we obtained a BaB_2O_4 single crystal of about 350 μm, which could further be used for X-ray diffraction analysis (Fig. 5a). Letter L in Fig. 5a denotes the region of partial melting (quenched melt). The obtained crystal is a *new high-pressure modification* of γ-BaB_2O_4, which is crystallized in the centrosymmetric space group $P2_1/n$, a = 4.6392(4) Å, b = 10.2532(14) Å, c = 7.066(1) Å, β = 91.363(10)°, Z = 4. The structure was added to the CCDC database, No. 2106970. A unique feature of the structure is the presence of the $[B_2O_6]$ group consisting of edge-sharing tetrahedra. The

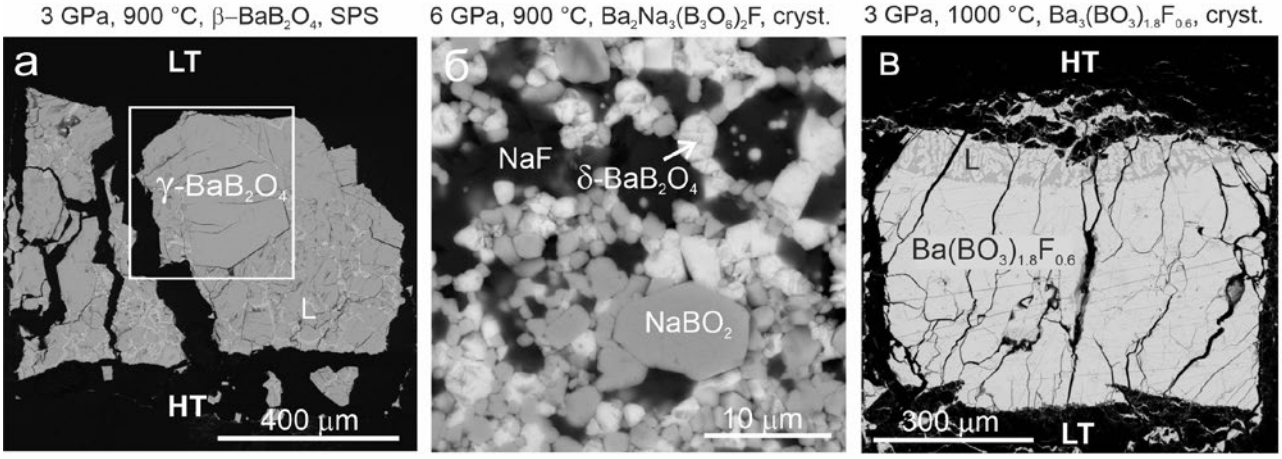

Fig. 5. Backscattered electron image of synthesis products under high pressure and temperature conditions: (a) synthesis at 3 GPa, 900 °C, initial sample – β-BaB_2O_4, obtained by solid-phase synthesis (SPS); (b) synthesis at 6 GPa, 900 °C, the initial sample is a ground crystal of $Ba_2Na_3[B_3O_6]_2F$; (c) synthesis at 3 GPa, 1000 °C, the initial sample is a ground crystal of $Ba_3(BO_3)_{1.8}F_{0.6}$. L – quenched melt, LT and HT – low and high temperature zones of the sample, respectively

metaborate ring disappears from the γ-BaB_2O_4 and two $_\infty[B_4O_4O_{8/2}]$ double endless chains appear along the *a* axis built of $[B_2O_6]$ groups connected by two $[BO_3]$ triangles. The γ-BaB_2O_4 phase is characterized by the shortest distance between the boron atoms of the edge-sharing tetrahedra, 1.984 Å, with the corresponding angles of 95.5° and 105.5° [24,48].

Edge-sharing tetrahedra were first discovered in 2002 in the $Dy_4B_6O_{15}$ compound synthesized at 8 GPa and 1000 °C by a group of researchers headed by professor Huppertz [49]. The discovery of edge-sharing tetrahedra led to the revision of one of the main rules of crystal chemistry of borates: it used to be considered that polymerization in borates takes place only at the vertices [50]. At the moment, there are a limited number of known structural types of borates with edge-sharing tetrahedra synthesized at high pressures by Prof. Huppertz's group [51, 52], as well as $KZnB_3O_6$ [53], $Li_4Na_2CsB_7O_{14}$ [54], $BaZnB_4O_8$ [55], and other compounds synthesized at atmospheric pressure. The theory of crystal chemistry of hard boron-oxygen groups formed by edge-sharing tetrahedra is only starting to develop, so there is little information yet about the properties of such compounds [56]. Thus, [54] states that $Li_4Na_2CsB_7O_{14}$ demonstrates an uncharacteristic anisotropy of a thermal expansion, $BaZnB_4O_8$ is characterized by both high birefringence $\Delta n = 0.14$ at a wavelength of 589.3 nm and a large band gap [55], while the $BaZnB_4O_8$: Tb^{3+}, Eu^{3+} phosphor based on it demonstrates outstanding thermal stability (90.2 % at 423 K) [57].

Based on the calculations, the fourth modification δ-BaB_2O_4 with the proposed structure $Pa\bar{3}$ isostructural to CaB_2O_4-$Pa\bar{3}$ [15], is stable under pressure above 6.1 GPa. In order to obtain δ-BaB_2O_4 crystals we conducted an experiment at a pressure of 6 GPa, which is the maximum pressure for the Discoverer-1500 multi-anvil hydraulic press of the DIE type. The initial samples were both β-BaB_2O_4 samples obtained by means of solid-phase synthesis and grounded crystals. The Raman spectra of the synthesized BaB_2O_4 crystals were identical to the spectra of γ-BaB_2O_4. However, we still managed to experimentally confirm the existence of the fourth modification δ-BaB_2O_4 when studying compound $Ba_2Na_3(B_3O_6)_2F$. When grounded $Ba_2Na_3(B_3O_6)_2F$ crystals were used as an initial sample at 6 GPa and 900 °C, the synthesized sample contained phases BaB_2O_4, $NaBO_2$, and NaF (Fig. 5b), which were identified by means of energy dispersive X-ray spectroscopy and Raman spectroscopy. At the same time, the $Ba_2Na_3(B_3O_6)_2F$ phase completely disappeared [27]. The small size of the formed crystals made it impossible to conduct X-ray diffraction studies. The results of the analysis of the synthesized BaB_2O_4 phase by means of Raman spectroscopy are presented in section 3.3.

For the first time we conducted experiments in order to study the stability of borates with an "antizeolite" structure under high pressures. When grounded $Ba_3(BO_3)_{1.8}F_{0.6}$ crystals were used as the initial sample at 3 GPa and 1000 °C, we obtained a single-phase sample of a similar composition, which had a region of partial melting (quenched melt) (Fig. 5c). The study determined that the compositions of the initial and synthesized samples were close, while their Raman spectra differed, which makes it possible to assume the presence of a phase transition that requires further research.

3.3. Raman spectra of polymorphic modifications of BaB_2O_4

Fig. 6 shows the Raman spectra of the four known polymorphic modifications of BaB_2O_4. The basis of the α-BaB_2O_4 ($R\bar{3}c$) [58] and β-BaB_2O_4 ($R3c$) structure [59] is a *metaborate* ring $[B_3O_6]^{3-}$, built of three triangles sharing a common vertex $[BO_3]$. The most intense vibration in the Raman spectra for metaborates traditionally corresponds to the so-called breathing mode of the metaborate ring, whose location practically does not depend on the composition of the compound. Thus, for α-BaB_2O_4 the vibration is registered at 634 cm^{-1} (Fig. 6a), for β-BaB_2O_4 – at 637 cm^{-1} (Fig. 6b), for $Ba_2Na_3[B_3O_6]_2F$ - at 628 cm^{-1} [27], and for $NaBO_2$ ($R\bar{3}c$) at 626 cm^{-1} [60].

The spectrum of β-BaB_2O_4 (Fig. 6b) is in good agreement with the previous studies, namely with [61], which describes out-of-plane modes at 58, 73, 99, 124, 172, and 197 cm^{-1}, and in-plane modes at 598, 620, 770, 788, 1499, 1526, and 1541 cm^{-1} of the metaborate ring $[B_3O_6]^{3-}$. In [62], the most intense peaks at 390, 498, and 620 cm^{-1} in the spectra of β-BaB_2O_4 at temperatures from 300 to

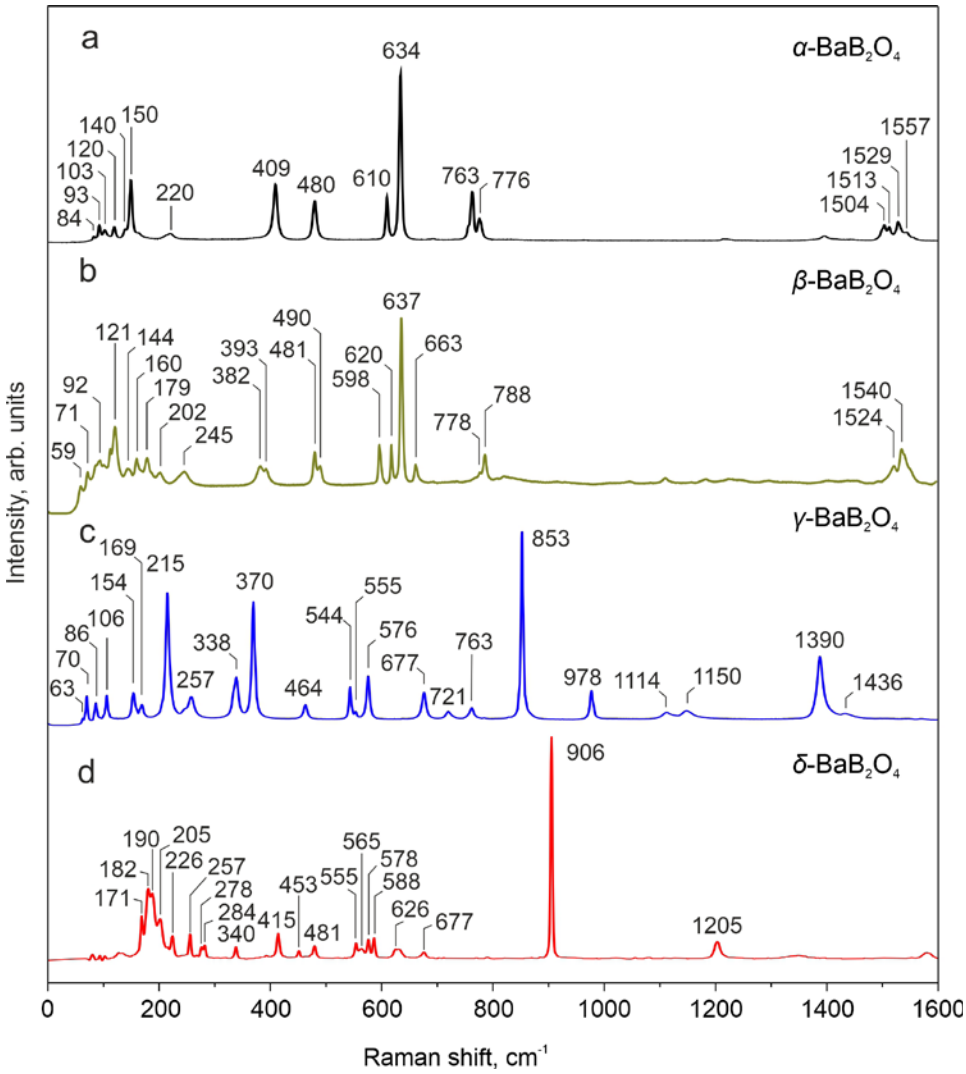

Fig. 6. Raman spectra of four polymorphs of BaB_2O_4

1100 K are attributed to the in-plane deformation vibrations of $[B_3O_6]^{3-}$; at higher temperatures the peaks monotonously move towards the region of lower frequencies.

The structure of γ-BaB_2O_4 ($P2_1/n$) includes double endless chains built of edge-sharing tetrahedra connected by $[BO_3]$-triangles [26]. Experimental and numerical studies of the Raman spectra demonstrated that the most intense band at 853 cm^{-1} corresponds to the breathing mode of the $^{(4)}B–O–^{(4)}B–O$ ring formed by two edge-sharing tetrahedra. Bands at 1436, 1390, 1150, and 1114 cm^{-1} correspond to stretching modes $^{(3)}B–O$. Bands in the range of 770–300 cm^{-1} are a combination of libration and deformation modes of groups $[BO_3]$ and $[BO_4]$, and bands below 300 nm – are combined out-of-plane libration and translation modes $[BO_3]$ of barium atoms and triangles. A more detailed study of the analyzed Raman spectra is presented in [26]. An analysis of the previous studies led us to a conclusion that the location and the intensity of the vibration corresponding to the breathing mode of the $^{(4)}B–O–^{(4)}B–O$ ring significantly depend on the structure of the boron-oxygen anionic complex *in general*. Thus, for $KZnB_3O_6$ the most intense vibration is registered at 723 cm^{-1} [52], and for HP-KB_3O_5 – at 760 cm^{-1} [51].

As we have mentioned earlier, we could not conduct X-ray diffraction studies of δ-BaB_2O_4 single crystals due to their small size. According to *ab initio* calculations, modification δ-BaB_2O_4 is

isostructural to CaB_2O_4-$Pa\bar{3}$ [15]. We can assume that the most intense vibration at 906 cm^{-1} is explained by the stretching vibrations of the $[BO_4]$ tetrahedron.

Numerical methods demonstrated that in the series $\alpha \rightarrow \beta \rightarrow \gamma \rightarrow \delta$ the band gap gradually increases (6.315 → 6.468 → 7.045 → 7.340 eV respectively). We should note that the calculated band gaps for the α- and β-BaB_2O_4 modifications are in good agreement with the experimental ones. The calculated *PT* phase diagram of BaB_2O_4 is presented in [48].

4. Conclusions

Based on the numerous studies of phase equilibria in the Na, Ba, B // O, F quaternary reciprocal system conducted in order to optimize the composition of the solvent used for the growth of β-BaB_2O_4 crystals, we can conclude that crystals of reproducibly good optical quality can be obtained when using compounds of systems BaB_2O_4 –$NaBaBO_3$ and BaB_2O_4 – $NaBaBO_3$ – $Ba_2Na_3[B_3O_6]_2F$. Using a Discoverer-1500 multi-anvil hydraulic press of the DIE type at high temperatures and pressures we synthesized two new polymorphic modifications: γ-BaB_2O_4 with a $P2_1/n$ structure (CCDC, № 2106970) and δ-BaB_2O_4 with a proposed structure $Pa\bar{3}$. A unique feature of the γ-BaB_2O_4 structure is the presence of the $[B_2O_6]$ group consisting of edge-sharing tetrahedra. Both modifications were analyzed using the Raman light scattering method.

The Na, Ba, B // O, F system also includes the region of compositions of the solid solution with an "antizeolite" structure. The composition of the solution in the system can be presented as $\{Ba_{12}(BO_3)_6\}[(F_2)_x(BO_3)_{1-x}][(F_4)_x(NaF_4)_y(BO_3)_{1-x-y}]$, where $x + y \leqslant 1$. Phases $Ba_3(BO_3)_2$, $Ba_3(BO_3)_{1.8}F_{0.6}$, and $NaBa_{12}(BO_3)_7F_4$ were experimentally determined. The crystals have dichroic properties that depend on the composition of the initial high-temperature solution; the dielectric permeability of $NaBa_{12}(BO_3)_7F_4$ is unusually high for borate crystals (319(5)). Raman spectroscopy determined that under high pressures $Ba_3(BO_3)_{1.8}F_{0.6}$ undergoes a phase transition, whose nature requires further research.

Author contributions

T. B. Bekker – idea, writing of the article, scientific editing of the text, experimental studies, head of the project; A. V. Davydov – experimental studies, project executor; N. E. Sagatov – numerical and experimental studies.

Conflict of interests

The authors declare that they have no known competing financial interests or personal relationships that could have influenced the work reported in this paper.

References

1. Chen C., Wu B., Jiang A., You G. A new-type ultraviolet SHG crystal – β-BaB_2O_4. *Materials Science, Physics Science in China Series B.*1985;28: 235–243. https://doi.org/10.1360/yb1985-28-3-235

2. Perlov D., Livneh S., Czechowicz P., Goldgirsh A., Loiacono D. Progress in growth of large β-BaB_2O_4 single crystals. *Crystal Research and Technology.* 2011;46: 651–654. https://doi.org/10.1002/crat.201100208

3. Mutailipu M., Poeppelmeier K. R., Pan S. Borates: A rich source for optical materials. *Chemical Reviews.*2021;121: 1130–1202. https://doi.org/10.1021/acs.chemrev.0c00796

4. Fedorov P. P., Kokh A. E., Kononova N. G., Barium borate beta-BaB_2O_4 as a material for nonlinear optics. *Russian Chemical Reviews* 2002;71(8): 651–671. https://doi.org/10.1070/RC2002v071n08ABEH000716

5. Chen C., Sasaki T., Li R., … Kaneda Y. *Nonlinear optical borate crystals, principles and applications*. Wiley-VCH Verlag GmbH & Co. KGaA; 2012. 387 p. https://doi.org/10.1002/9783527646388

6. Feigelson R. S., Raymakers R. J., Route R. K. Solution growth of barium metaborate crystals by top seeding. *Journal of Crystal Growth.* 1989;97: 352–366. https://doi.org/10.1016/0022-0248(89)90217-0

7. Nikolov V., Peshev P. On the growth of β-BaB_2O_4 (BBO) single crystals from hightemperature solutions: I. Study of solvents of the BaO–Na_2O–B_2O_3 system. *Journal of Solid State Chemistry.* 1992;96: 48–52. https://doi.org/10.1016/S0022-4596(05)80295-6

8. Tang D.Y., Zeng W. R., Zhao Q. L. A study on growth of β-BaB_2O_4 crystals. *Journal of Crystal Growth.* 1992;123: 445–450. https://doi.org/10.1016/0022-0248(92)90605-I

9. Fedorov P. P., Kokh A. E., Kononova N. G., Bekker T. B. Investigation of phase equilibria and growth of BBO (β-BaB_2O_4) in BaO-B_2O_3-Na_2O ternary system. *Journal of Crystal Growth.* 2008;310: 1943–1949. https://doi.org/10.1016/j.jcrysgro.2007.11.119

10. Roth M., Perlov D. Growth of barium borate crystals from sodium fluoride solutions, *Journal of Crystal Growth*. 1996;169: 734–740. https://doi.org/10.1016/S0022-0248(96)00450-2

11. Chen W., Jiang A., Wang G. Growth of high-quality and large-sized β-BaB_2O_4 crystal. *Journal of Crystal Growth.* 2003;256: 383–386. https://doi.org/10.1016/S0022-0248(03)01358-7

12. Perlov D., Livneh S., Czechowicz P., Goldgirsh A., Loiacono D. Progress in growth of large β-BaB_2O_4 single crystals. *Crystal Research and Technology*. 2011;46: 651–654. https://doi.org/10.1002/crat.201100208

13. Bekker T. B., Kokh A. E., Kononova N. G., Fedorov P. P., Kuznetsov S. V. Crystal growth and phase equilibria in the BaB_2O_4–NaF system. *Crystal Growth and Design*. 2009;9: 4060–4063. https://doi.org/10.1021/cg9002675

14. Sagatov N. E., Bekker T. B., Podborodnikov I. V., Litasov K. D. First-principles investigation of pressure-induced structural transformations of barium borates in the BaO–B_2O_3–BaF_2 system in the range of 0–10 GPa. *Computational Materials Science*. 2021;199: 110735. https://doi.org/10.1016/j.commatsci.2021.110735

15. Marezio M., Remeika J. P., Dernier P. D. The crystal structure of the high-pressure phase CaB_2O_4 (IV), and polymorphism in CaB_2O_4. *Acta Crystallographica B*. 1969;25: 965–970. https://doi.org/10.1107/S0567740869003256

16. Bekker T. B., Fedorov P. P., Kokh A. E. Phase formation in the BaB2O4 -BaF2 system. *Crystallogr. Rep*. 2012;57(4): 574–578. https://doi.org/10.1134/S1063774512040025

17. Jiang A., Cheng F., Lin Q., Cheng G., Zheng Y. Flux growth of large single crystals of low temperature phase barium metaborate. *Journal of Crystal Growth*. 1986;79: 963–969. https://doi.org/10.1016/0022-0248(86)90579-8

18. Bekker T. B., Kokh A. E., Fedorov P. P. Phase equilibria and beta-BaB_2O_4 crystal growth in the BaB_2O_4-BaF_2 system. *CrystEngComm*. 2011;13: 3822–3826. https://doi.org/10.1039/C1CE05071K

19. Jänecke E. Über reziproke Salzpaare und doppeltternäre Salzmischungen, *Zeitschrift für Physikalische Chemie*. 1913;82: 1–34. https://doi.org/10.1515/zpch-1913-8202

20. Tu J. -M. Keszler D. A. $BaNaBO_3$. *Acta Crystallographica*.1995;51(10): 1962–1964. https://doi.org/10.1107/s010827019400750x

21. Kokh A.E., Kononova N.G., Bekker T. B., Fedorov P.P., Nigmatulina E.A., Ivanova A.G. An investigation of the growth of β-BaB_2O_4 crystals in the BaB_2O_4-NaF system and new fluoroborate $Ba_2Na_3[B_3O_6]_2F$. *Crystallogr. Rep*. 2009;54(1): 146–151. https://doi.org/10.1134/S1063774509010258

22. Bekker T. B., Rashchenko S. V., Solntsev V. P., … Kuznetsov A. B. Growth and optical properties of $Li_xNa_{1-x}Ba_{12}(BO_3)_7F_4$ fluoride borates with 'anti-zeolite' structure. *Inorganic Chemistry*. 2017;56(9): 5411–5419. https://doi.org/10.1021/acs.inorgchem.7b00520

23. Bekker T. B., Rashchenko S. V, Seryotkin Y. V., Kokh A. E., Davydov A. V., Fedorov P. P. BaO–B_2O_3 system and its mysterious member $Ba_3B_2O_6$. *Journal of the American Ceramic Society*. 2018;101(1): 450–457. https://doi.org/10.1111/jace.15194

24. Rashchenko S. V., Bekker T. B., Bakakin V. V., Seryotkin Y. V., Simonova E. A., Goryainov S. V. New fluoride borate with 'anti-zeolite' structure: A possible link to $Ba_3(BO_3)_2$. *Journal of Alloys and Compounds*. 2017;694: 1196–1200. https://doi.org/10.1016/j.jallcom.2016.10.119

25. Zhao J., Li R. K. Two new barium borate fluorides ABa_{12} $(BO_3)_7F_4$ (A= Li and Na). *Inorganic Chemistry*. 2014;53(5): 2501-2505. https://doi.org/10.1021/ic4025525

26. Bekker T. B., Podborodnikov I. V., Sagatov N. E., … Litasov K. D. γ-BaB_2O_4: high-pressure high-temperature polymorph of barium borate with edge-sharing BO_4 tetrahedra. *Inorganic Chemistry*. 2022;61(4): 2340–2350. https://doi.org/10.1021/acs.inorgchem.1c03760

27. Sagatov N. E., Bekker T. B., Vinogradova Y. G., Davydov A. V., Podborodnikov I. V., Litasov K. D. Experimental and ab initio study of $Ba_2Na_3(B_3O_6)_2F$ stability in the pressure range of 0–10 GPa. *International Journal of Minerals, Metallurgy and Materials*. 2023;30(9): 1846–1854. https://doi.org/10.1007/s12613-023-2647-0

28. Shatskiy A., Sharygin I. S., Gavryushkin P. N., … Ohtani E. The system K_2CO_3-$MgCO_3$ at 6 GPa and 900-1450 °C. *American Mineralogist*. 2013;98(8-9): 1593–1603. https://doi.org/10.2138/am.2013.4407

29. Bekker, T. B., Fedorov, P. P. New type of ternary reciprocal system: Na,Ba//BO_2,F system. *Russian Journal of Inorganic Chemistry*. 2014;59: 1507–1511. https://doi.org/10.1134/S0036023614120055

30. Bekker T. B., Fedorov P. P., Kokh A. E. The ternary reciprocal system Na, Ba // BO_2, F. *Crystal Growth and Design*. 2012;12(1): 129–134. https://doi.org/10.1021/cg2008705

31. Huang Q. -Z., Liang J. K. The crystal growth of barium borate low temperature phase and the study of phase diagrams of related systems. *Acta Physica Sinica* 1981;30: 559. (In Chinese). https://doi.org/10.7498/aps.30.559

32 Furmanova, N. G., Maksimov, B. A., Molchanov, V. N., Kokh A. E., Kononova N. G., Fedorov P. P. Crystal structure of the new barium borate $Ba_5(BO_3)_2(B_2O_5)$. *Crystallography Reports*. 2006;51: 219–224. https://doi.org/10.1134/S1063774506020076

33. Kokh A. E., Kononova N. G., Bekker T. B., … Kargin Yu. F. New sodium barium orthoborate $NaBa_4(BO_3)_3$. *Russian Journal of Inorganic Chemistry*. 2004;49(7): 984–988.

34. Bekker T. B. *Phase formation and crystal growth in the quaternary reciprocal system Na, Ba, B // O, F**. Dissertation of Dr. Geol.-miner. Sci. Novosibirsk: 2015. 279 p. https://www.dissercat.com/content/fazoobrazovanie-i-rost-kristallov-v-chetvernoi-vzaimnoi-sisteme-na-ba-b-o-f

35. Bekker T. B., Fedorov P. P., Kokh A. E. Phase formation and crystal growth in the quaternary reciprocal system Na, Ba, B // O, F. Novosibirsk: Siberian Branch of the Russian Academy of Sciences Publ. 2016. 217 p. (In Russ.). Available at: https://www.rfbr.ru/library/books/2416/

36. Carrillo Romo F., Goutaudier C., Guyot Y., Cohen-Adad M. Th., Boulon G., Lebbou K., Yoshikawa A., Fukuda T. Yb^{3+}-doped $Ba_2NaNb_5O_{15}$ (BNN) growth, characterization and spectroscopy. *Optical Materials*. 2001;16: 199–206. https://doi.org/10.1016/S0925-3467(00)00078-1

37. Hong W., Perlov D., Halliburton L. E. Electron paramagnetic resonance study of Ag^0 atoms and Ag^{2+} ions in β-BaB_2O_4 nonlinear optical crystals. *Journal of Physics D: Applied Physics*. 2003;36: 2605–2611. https://doi.org/10.1088/0022-3727/36/21/002

38. Hong W., Halliburton L. E., Perlov D., Stevens K. T., Route R. K., Feigelson R. S. Observation of paramagnetic point defects in BBO (β-BaB_2O_4) crystals. *Optical Materials*. 2004;26(4): 437–441. https://doi.org/10.1016/j.optmat.2003.08.012

39. Bekker T. B., Kokh A. E., Fedorov P. P., Stonoga S. Yu. Phase equilibria and growth of β-BaB_2O_4 crystals in the BaB_2O_4-$Ba_2Na_3[B_3O_6]_2F$ system. *Crystallography Reports*. 2012;57(2): 327–331. https://doi.org/10.1134/s1063774512020022]

40. Fedorov P. P., Kokh A. E., Kononova N. G., Bekker T. B. Investigation of phase equilibria and growth of BBO (β-BaB_2O_4) in BaO-B_2O_3-Na_2O ternary system. *Journal of Crystal Growth*. 2008;310(7-9): 1943–1949. https://doi.org/10.1016/j.jcrysgro.2007.11.119

41. Palacios L., Cabeza, A., Bruque S., García-Granda S., Aranda M. A. Structure and electrons in mayenite electrides. *Inorganic Chemistry*. 2008;47(7): 2661–2667. https://doi.org/10.1021/ic7021193

42. Kim S. W., Hosono H. Synthesis and properties of $12CaO·7Al_2O_3$ electride: review of single crystal and thin film growth. *Philosophical Magazine*. 2012;92(19-21): 2596-2628. https://doi.org/10.1080/14786435.2012.685770

43. Zhang X., Feng Q., Zhao J., … Lu Q. Sr-doping enhanced electrical transport and thermionic emission of single crystal $12CaO·7Al_2O_3$ electride. *Current Applied Physics*. 2020;20(1): 96–101. https://doi.org/10.1016/j.cap.2019.10.008

44. Li R., Zhang X., Xiao Y., Liu Y. One-step preparation and electrical transport characteristics of single-crystal $Ca_{24}Al_{28}O_{66}$ electrides. *Journal of Electronic Materials*. 2020;49: 7308–7315. https://doi.org/10.1007/s11664-020-08469-0

45. Bekker T. B., Solntsev V. P., Rashchenko S. V., … Park S.-H. Nature of color of the borates with the 'anti-zeolite' structure. *Inorganic Chemistry*. 2018;57(5); 2744–2751. https://doi.org/10.1021/acs.inorgchem.7b03134

46. Bekker T. B., Solntsev V. P., Eliseev A. P., … Kuznetsov A. B. *Dichroic material – fluoride borate with an "anti-zeolite" structure**. Russian Federation Patent RF: No. 2689596. Publ. 05.28.2019, bull. No. 16. (In Russ.)]

47. Bekker T. B., Khamoyan A. G., Davydov A. V., Vedenyapin V. N., Yelisseyev A. P., Vishnevskiy A. V. $NaBa_{12}(BO_3)_7F_4$ (NBBF) dichroic crystals: optical properties and dielectric permittivity. *Dalton Transactions*. 2024; 53(29): 12215-12222. https://doi.org/10.1039/d4dt01380h

48. Bekker T. B., Davydov A. V., Sagatov N. E. Comparative characteristics of various solvents of the Na, Ba, B//O, F system for the growth of β-BaB_2O_4 crystals and PT-diagram of BaB_2O_4 polymorphs. *Journal of Crystal Growth*. 2022;599: 126895. https://doi.org/10.1016/j.jcrysgro.2022.126895

49. Huppertz H., von der Eltz B. Multianvil high-pressure synthesis of $Dy_4B_6O_{15}$: the first oxoborate with edge-sharing BO_4 tetrahedra. *Journal of the American Chemical Society*. 2002;124(32): 9376-9377. https://doi.org/10.1021/ja017691z

50. Grice J. D., Burns P. C., Hawthorne F. C. Borate minerals. II. A hierarchy of structures based upon the borate fundamental building block. *The Canadian Mineralogist*. 1999;37(3): 731–762.

51. Knyrim J. S., Roessner F., Jakob S., … Huppertz H. Formation of edge-sharing BO_4 tetrahedra in the high-pressure borate HP-NiB_2O_4. *Angewandte Chemie International Edition*. 2007;46(47): 9097–9100. https://doi.org/10.1002/anie.200703399

52. Neumair S. C., Vanicek S., Kaindl R., … Huppertz H. HP-KB_3O_5 highlights the structural diversity of borates: corner-sharing BO_3/BO_4 groups in combination with edge-sharing BO_4 tetrahedra. *European Journal of Inorganic Chemistry*. 2011;27: 4147–4152. https://doi.org/10.1002/ejic.201100618

53. Jin S., Cai G., Wang W., He M., Wang S., Chen X. Stable oxoborate with edge-sharing BO_4 tetrahedra synthesized under ambient pressure. *Angewandte Chemie International Edition*. 2010;122(29): 5087–5090. https://doi.org/10.1002/ange.200907075

54. Mutailipu M., Zhang M., Li H., … Pan S. $Li_4Na_2CsB_7O_{14}$: a new edge-sharing $[BO_4]_5$–tetrahedra containing borate with high anisotropic thermal expansion. *Chemical Communications*. 2019;55(9): 1295–1298. https://doi.org/10.1039/c8cc09422e

55. Han J., Liu K., Chen L., … Mutailipu M. Finding a deep-UV borate $BaZnB_4O_8$ with edge-sharing $[BO_4]$ tetrahedra and strong optical anisotropy. *Chemistry – A European Journal*. 023;9(6): 202203000. https://doi.org/10.1002/chem.202203000

56. Li J. J., Chen W. F., Lan Y. Z., Cheng J. W. Recent progress in crystalline borates with edge-sharing BO_4 tetrahedra. *Molecules*. 2023;28(13): 5068. https://doi.org/10.3390/molecules28135068

57. Liu N., Kong J., Wang Z., Wang Y. Color-tunability and energy transfer of a highly thermal-stable $BaZnB_4O_8$: Tb^{3+}/Eu^{3+} phosphor for single-component w-LEDs. *Journal of Molecular Structure*. 2024;1311: 138441. https://doi.org/10.1016/j.molstruc.2024.138441

58. Mighell A. D., Perloff A., Block S. The crystal structure of the high temperature form of barium borate, $BaO·B_2O_3$. *Acta Crystallographica*. 1966;20: 819–823. https://doi.org/10.1107/S0365110X66001920

59. Bubnova R., Volkov S., Albert B., Filatov S. Borates – crystal structures of prospective nonlinear optical materials: high anisotropy of the thermal expansion caused by anharmonic atomic vibrations. *Crystals*. 2017;7(3): 93. https://doi.org/10.3390/cryst7030093

60. Voronko Yu. K., Sobol A. A., Shukshin V. E. Structure of boron-oxygen fragments of metaborates of alkali and alkaline earth metals in crystalline, molten and glassy states. *Inorganic materials*. 2012:48(7); 837. (In Russ.). Available at: https://www.elibrary.ru/item.asp?id=17745523

61. Lu J. Q., Lan G. X., Li B., Yang Y. Y., Wang H. F., Bai C. W. Raman scattering study of the single crystal β-BaB_2O_4 under high pressure. *Journal of Physics and Chemistry of Solids*. 1988;49(5): 519–527. https://doi.org/10.1016/0022-3697(88)90063-7

62. Liu S., Zhang G., Wan S., … Wu Y. High-temperature Raman spectroscopy of microstructure around the growing β-BaB_2O_4 crystal in the BaO–B_2O_3–Na_2O system. *Journal of Applied Crystallography*. 2014;47(2): 739-744. https://doi.org/10.1107/S160057671400377X

**Translated by author of the article*

Information about the authors

Tatyana B. Bekker, Dr. Sci. (Geol.-Mineral.) Leading Researcher, Sobolev Institute of Geology and Mineralogy, Siberian Branch of Russian Academy of Sciences, (Novosibirsk, Russian Federation), Senior Research Worker of Novosibirsk State University (Novosibirsk, Russian Federation).
https://orcid.org/0000-0003-3100-5210
bekker@igm.nsc.ru, t.b.bekker@gmail.com

Nursultan E. Sagatov, Cand. Sci. (Phys.- Math.), Researcher Fellow, Sobolev Institute of Geology and Mineralogy, Siberian Branch of Russian Academy of Sciences, (Novosibirsk, Russian Federation), Novosibirsk State University (Novosibirsk, Russian Federation).
https://orcid.org/0000-0001-5158-3523
sagatovnye@igm.nsc.ru

Aleksey V. Davydov, Researcher, Sobolev Institute of Geology and Mineralogy, Siberian Branch of Russian Academy of Sciences, (Novosibirsk, Russian Federation), Novosibirsk State University (Novosibirsk, Russian Federation).
https://orcid.org/0000-0003-2770-3331
adavidov@igm.nsc.ru, a.davydov1@nsu.ru

Received 01.07.2024; approved after reviewing 08.07.2024; accepted for publication 16.09.2024; published online 25.12.2024.

Translated by Yulia Dymant